Int. J. Electrochem. Sci., 10 **(2015)** 9154 - 9166

International Journal of
ELECTROCHEMICAL
SCIENCE
www.electrochemsci.org

Anticorrosive Properties of Oligoaniline Containing Photo-cured Coatings

Bin Chen[1], Jun Ma[1,2] , Lin Gu[2], Shuan Liu[2,], Haichao Zhao[2,*], Haibin Yu[2], Jianmin Chen[2]*

[1] School of Materials Science and Engineering, Shenyang University of Chemical Technology, 11 St. Economic & Technological Development Zone, Shenyang 110142, P. R. China.
[2] Key Laboratory of Marine Materials and Related Technologies, Zhejiang Key Laboratory of Marine Materials and Protective Technologies, Ningbo Institute of Materials Technology and Engineering, Chinese Academy of Sciences, Ningbo 315201, P. R. China.
*E-mail: shuanliu312@163.com, zhaohaichao@nimte.ac.cn

Received: 17 July 2015 / *Accepted:* 31 August 2015 / *Published:* 30 September 2015

Electro-active maleic acid capped trianiline (MTA) was synthesized by reaction of maleic anhydride with trianiline (TA). Photopolymerization of aromatic acrylate (PAA) and MTA were applied on Q235 carbon steel to afford oligoaniline containing electroactive coatings. The anticorrosion behavior of photo-cured coatings with 1 wt% and 2.5 wt% MAT was investigated in 3.5% NaCl solution via potentiodynamic polarization curves and electrochemical impedance spectroscopy (EIS). It was observed that acrylate containing MTA coatings exhibited better corrosion resistance than the pure aromatic acrylate coating did.

Keywords: UV-curable, acrylate coatings, trianiline, anticorrosion

1. INTRODUCTION

Since Deberry reported stainless steels covered by a thin polyaniline (PANI) film exhibited an excellent corrosion resistance in an acidic environment in 1985 [1], interest has been increasing in the use of intrinsically conducting polymers (ICPs) for the protection of metallic materials against corrosion [2, 3]. Among all the ICPs, PANI is one of the most studied conducting polymers for anticorrosion applications because of its ease of synthesis, environmental stability and relative low cost [4]. One of the most convenient ways to prepare PANI based anticorrosive coatings is via direct electropolymerization on the metallic substrate [5-7]. However, electrodeposited PANI suffered from some disadvantages such as limited mechanical properties, poor adhesion to the metal surface, and poor processability, which restricts its further practical applications.

An alternative strategy for achieving PANI based anticorrosive coatings is the addition of miscible or dispersible PANI nanoparticles to the conventional polymeric resins to obtain composite coatings. This technology combines the electrochemical protection of metal from PANI and the good barrier protection from polymeric resins, enabling the enhancement of anticorrosion performance via synergistic effects between PANI and polymeric resins. To present, a variety of PANI-based nanoparticles has also been developed as anticorrosive additives for the organic coatings including proton acid doped PANI nanoparticles [8] and PANI hybrid composites (typically with SiO_2 [9-11], Clay [12, 13], ZnO [14], Zn [15], glass fiber [16], Al_2O_3 [17], carbon nanotube [18], grahite [19], graphene [20].

Oligoanilines analogues such as trianiline, tetraaniline and pentaaniline exhibit similar electrochemical properties as PANI. Meanwhile, the solubility of oligoanilines is much improved over that of PANI [21, 22]. Several oligoaniline-containing anticorrosive coatings have been developed, including epoxy thermosets [23, 24], polyimide [25, 26], polyurea [27], thermal-cured maleimide-containing benzoxazine and amine-capped aniline trimmer [28]. The preparation of anticorrosive polyimide/clay and polyimide/graphene hybrid coatings has also been reported by Yeh and coworkers [29]. Remarkably enhanced corrosion protection on metal was observed due to synergistic effects of electroactive aniline trimer and barrier properties of clay and graphene. Recently, we have prepared oligoaniline-containing electroactive hybrid coatings by sol-gel reaction of *N*-(3-triethoxysilylpropylureido) anilinetetramer (TESPAT) and triethoxymethylsilane (TEMS). The as-prepared hybrid coatings exhibited remarkably improved corrosion protection of steel as confirmed by polarization curves and electrochemical impedance spectroscopic (EIS) measurements [30].

Recently, photoinduced polymerization has drawn much attention in the field of organic coatings because it processes many advantages such as fast curing speed, low energy consumption and low VOC content[31]. Up to now, there is no report on utilization of photo curing technique to prepare oligoaniline-based anticorrosive coatings. In this study, we demonstrated the synthesis of novel maleic acid-capped trianiline (MTA), and preparation of anticorrosive coatings on Q235 carbon steel via photopolymerization of aromatic acrylate and maleic acid capped trianiline (MTA) in presence of phosphorus photoinitiator (Figure 1). The anticorrosion behavior of the composite coatings was studied by potentiodynamic polarization curves and electrochemical impedance spectroscopy (EIS).

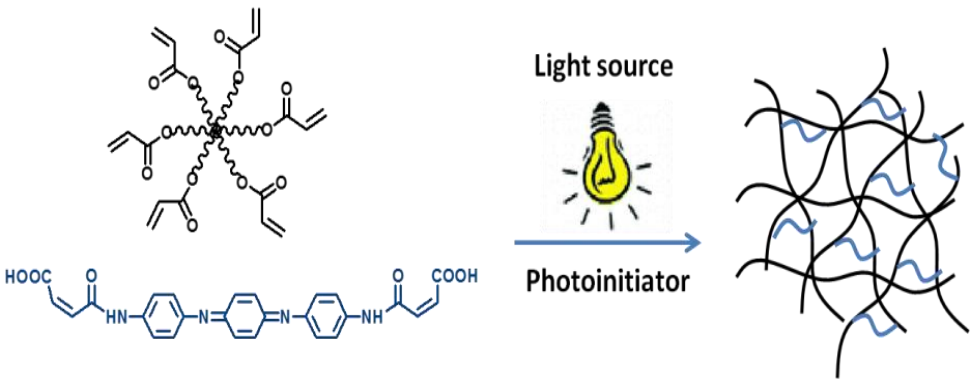

Figure 1. Preparation of electroactive coatings by photocuration of hexafunctional acrylate and maleic acid-capped trianiline (MTA).

2. EXPERIMENTAL

2.1 Materials

All reagents were purchased from Sigma-Aldrich and Aladdin, and used without further purification unless otherwise noted. UV-curable aromatic acrylate (AA, Hexafunctional SARTOMER CN975 NS, molecular weight of approx. 800) was donated from SARTOMER Company. The aniline trimer was prepared according to the literature [32].

2.2 Synthesis of Maleic Acid-Caped Aniline Trimer (MTA)

Maleic acid-caped aniline trimer (MTA) was synthesized by reaction of trianiline with maleic anhydride in THF at 40 ^{o}C. Typically, aniline trimer (2.90 g, 10 mmol) and maleic anhydride (2.45 g, 25 mmol) were dissolved in THF (40 mL) with vigorous stirring at 40 °C. After the reaction was carried out for 5 h at 50 ^{o}C, the mixture was precipitated from a large amount of petroleum ether. The solid was collected by filtration, purified by reprecipitation from THF into petroleum ether, and dried at 60 °C in vacuum to yield 3.9 grams of MTA (80.3%).

2.3Preparation of UV-curing composite coatings

Q235 carbon steel was used for all the electrochemical studies. The steel specimens were used as working electrode, and they were embedded in epoxy resin with a surface area of 1.0 cm^2 exposed. The specimens were carefully abraded with sequence emery papers of various grade (400-800 grit), washed with distilled water, degreased in acetone, and finally dried in a vacuum. MTA (1 wt% or 2.5 wt%), diphenyl (2,4,6-trimethylbenzoyl)-phosphine oxide (photoinitiator, 0.5 wt%), and aromatic urethane acrylate were predissolved in THF and stirred for 1 hour to form a homogenous solution. After the solvent was removed by rotary evaporator, the liquid prepolymer mixtures were applied on the Q235 steel electrode surfaces with a bar coater with a coating thickness about 20 μm measured using a PosiTector6000FNS1 apparatus. The coated electrode was then exposed to UV light (365 nm, 1 kw) for 3 minutes to obtain PAA/MTA coatings. Pure PAA coating was also prepared in a similar procedure except the addition of MTA.

2.4 Characterizations

The chemical structure of maleic acid capped trianiline (MTA) was identified by FTIR(NICOLET 6700, Thermo), ^{1}H NMR (400 MHz AVANCE III, Bruker) and UV-vis spectra (Lambda 950, Perkin-Elmer), respectively. For FTIR, MTA was analyzed using the KBr pellet method, the background spectrum was obtained from a pure KBr pellet of the same size. Cyclic voltammetry (CV) measurement of MTA was carried out in a conventional three-electrode cell with a platinum counter electrode and a saturated calomel electrode (SCE) equipped with a Luggin capillary as reference. MTA modified glassy carbon electrode was working electrode.

Electrochemical impedance spectroscopy (EIS) and polarization curves were performed on an electrochemical workstation (CHI-660E, Chenhua) in 3.5 wt% NaCl solution at room temperature. Before corrosion test, the open circuit potential (OCP) was measured, then the EIS measurements were performed at OCP with a 15 mV AC perturbation in the frequency range of 10^5 Hz to 0.01 Hz. To quantitatively evaluate the anticorrosive performance of as-prepared composite coatings, the EIS data were fitted by ZsimpWin3.21 software with equivalent circuits. Polarization curves were recorded from -250 mV to +250 mV versus OCP by changing the electrode potential automatically with a scan rate of 0.5 mV/s.

3. RESULT AND DISCUSSION

3.1 Synthesis and characterization of maleic acid capped trianiline (MTA)

The preparation of photoactive oligoaniline is shown in Scheme 1. Reaction of excess maleic anhydride with trianiline afforded maleic acid capped trianiline (MTA) in 80.3% yield. The structure of MTA was characterized by FTIR and NMR spectroscopy. In the FTIR spectrum of trianiline (TA) (Figure 2), the characteristic absorption bands at 3311and 3209 cm^{-1} are assigned to terminal NH_2 of trianiline, and the absorption bands appearing at 1599 and 1498 cm^{-1} arise from the vibrational bands of the quinoid rings and benzenoid rings of trianiline, respectively. The absorption peaks at 1303 cm^{-1} and 827 cm^{-1} are characteristic of the aromatic N-H group and the benzene ring. For the FTIR spectrum of MTA, the NH_2 absorption bands at 3311 and 3209 cm^{-1} were almost disappeared due to the reaction of malic anhydride. In the mean time, the presence of C=O and C=C absorbance peaks at 1706, 1694 and 1640 cm^{-1} confirmed the successful reaction between maleic anhydride and aniline trimer.

For further NMR spectroscopy characterizations (Figure 3), the signals appearing at 5.5 ppm are attributed to the primary amine protons of TA, and signals at around 7.0 ppm represent the aromatic proton signals. The complete reaction between TA and malice anhydride was confirmed by the disappearance of primary amine protons at 5.5 ppm, accompanying the presence of typical carboxylic acid protons (10.5 ppm), primary amide protons (7.8 ppm), and double bond protons (6.2 and 6.4 ppm) derived from end capped maleic acid.

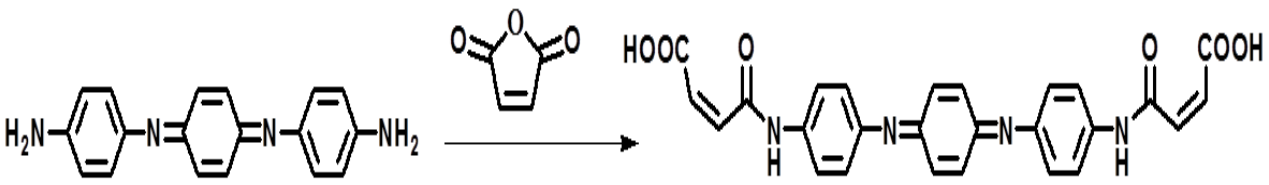

Scheme 1. Synthesis of maleic acid-capped trianiline

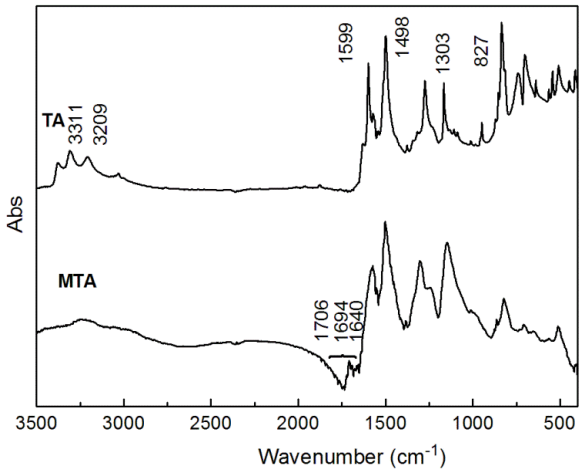

Figure 2. FTIR spectra of TA and MTA.

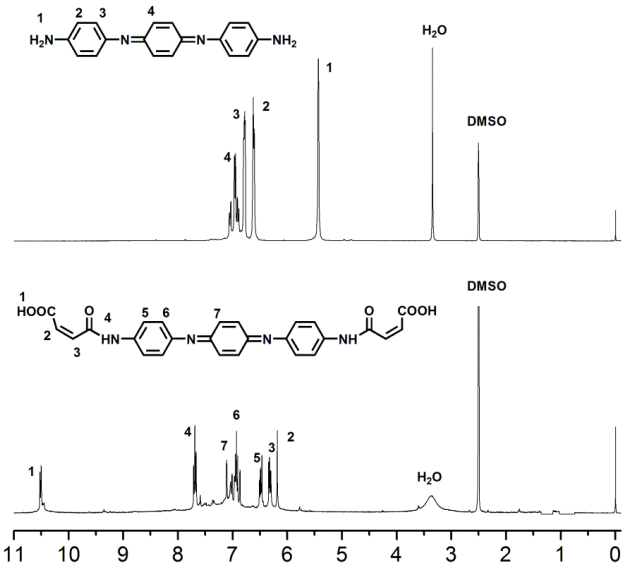

Figure 3. [1]H NMR spectra of trianiline and MTA measured in DMSO-*d6*.

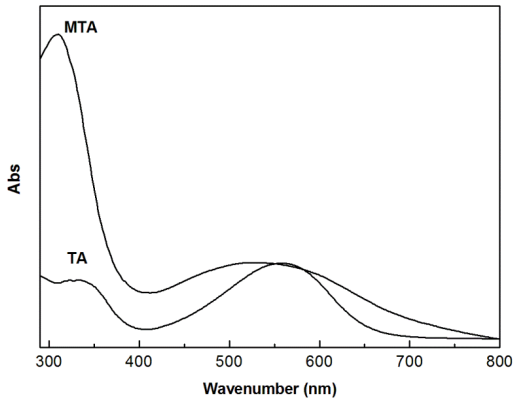

Figure 4. UV-vis spectra of TA and MTA measured in THF.

3.2 Electro-optical Properties of MTA

The electro-optical properties of MTA were confirmed by UV-vis spectra and cyclic voltammetry (CV). As can be seen from Figure 4, TA and MTA show similar UV-vis absorptions to those of undoped polyanilines, which exhibit two absorption maxima at around 320 and 550 nm. These peaks represent the π-π* transition benzenoid ring and charge-transfer excitation-like transition bands of the emeraldine base form of oligoaniline. Cyclic voltammetry (CV) measurement of MTA was conducted in 1 M HCl as a scan rate of 20 mV/s. It showed a single oxidation peak with an oxidation current of 66 μA/cm^2, and an reduction peak with a reduction current of 84μA/cm^2 (Figure 5a), which is similar to the reported trianiline derivatives that undergo a two electron transfer processes[23] (Figure 5b).

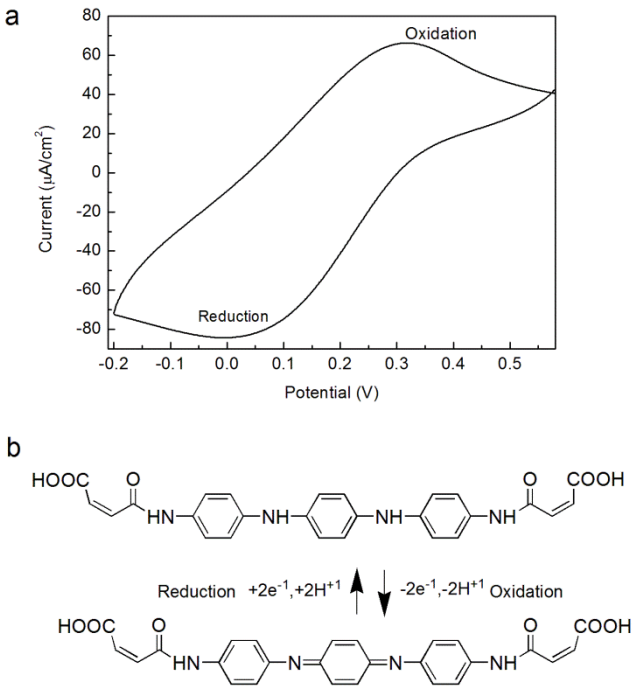

Figure 5. Redox behavior of MTA modified glassy carbon electrode measured in 1.0 M HCl aqueous solution, the scan rate was 20 mV/s.

3.3 Preparation and Characterization of UV-cured AUA/MTA composite coatings

The use of photocurable materials for coating applications is advantageous because it is eco-friendly and energy-efficient compared to traditional solvent-based processes. In present study, incorporation of MTA (1 wt% and 2.5 wt%) into liquid hexafunctional aromatic acrylate and subsequent photopolymerization afforded oligoaniline containing electroactive coatings. The composite coatings were characterized by FTIR and SEM. As shown in Figure 6, the typical absorption bands of acrylate monomer at 1727, 1635 and 810 cm^{-1} are assigned to C=O stretching, C=C vibration and =CH alkene twisting absorptions, respectively. After the acrylate/MTA precursor

were exposed to UV light for 3 minutes, the significant weakness of the absorption peaks at 1635 and 810 cm^{-1} confirmed the occurrence of photopolymerization. The morphology of as prepared acrylate/MTA coating surface or cross section showed no obvious phase separation or coating defect as evidenced by SEM (Figure 7).

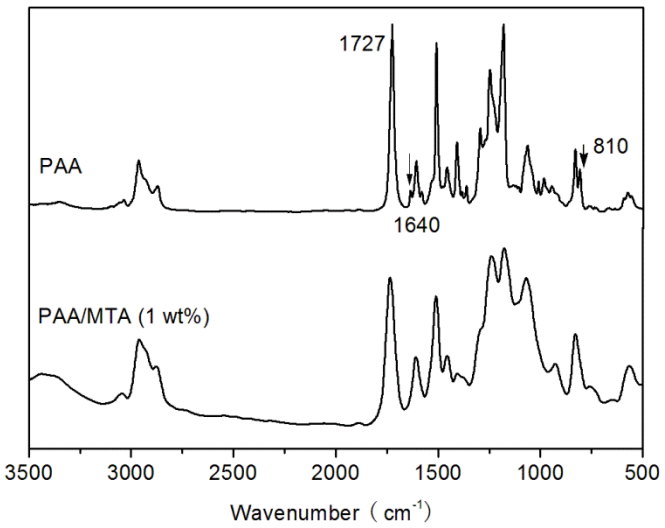

Figure 6. FTIR spectra of PAA and PAA/ 1% MTA coatings

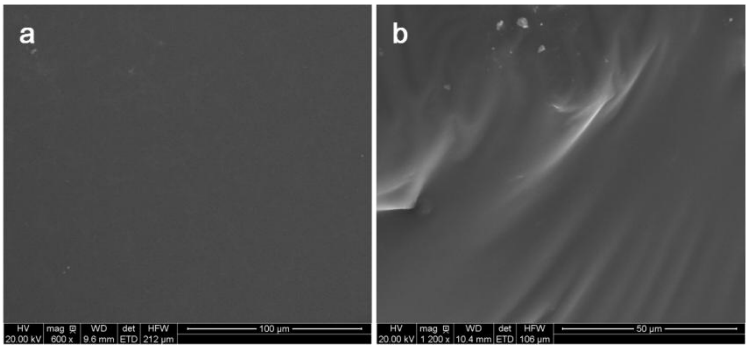

Figure 7. SEM images of (a) surface morphology of PAA/ 1% MTA coating and (b) cross-section of PAA/ 1% MTA coating.

3.4 Potentiodynamic Measurements

PANI has been widely used for corrosion protection of metals such as carbon steel [33], titanium[34], copper[35] and aluminum alloys[36]. However, the poor solubility and processability of polyaniline limited its further applications as anticorrosion coatings. To address this issue, considerable work has recently been done by incorporation of oligoanilines into synthetic polymers. Such oligoaniline-based base polymers exhibit improved solubility, while maintaining similar electrochemical properties as PANI due to their conjugated structures. [37]. We therefore anticipated

that this redox behavior of MTA based photocured coatings exhibit a similar enhanced anticorrosive performance, as confirmed by polarization curves and EIS.

Figure 8 shows the Tafel polarization curves for bare *Q*235 steel, steel coated with pure acromatic acrylate coatings (PAA), steel coated PAA coating with 1.0% and 2.5 wt% MAT after 48 hours immersion in 3.5% NaCl solution. The Tafel region are identified (±50mV with respect to the corrosion potential) and the corrosion current density (i_{corr}), corrosion potential (E_{corr}) are determined by superimposing a straight line along the linear portion of the cathodic and anodic curves [38]. The corrosion rate of bare Q235 steel decreased obviously when it coated with different composite coatings as seen in Table 1. Compare to the neat PAA coating (-0.635V), the shift in the E_{corr} towards more positive values for the PAA/1.0%wt MTA (-0.614V) and PAA/2.5% wt MTA (-0.601V) are apparent after 48 hours of exposure. The i_{corr} of PAA-2.5%MTA is only 0.082 μA cm^{-2} after immersed in 3.5% NaCl solution after 48 hours, which is lowered 200 times than of the bare Q235 steel (17.1 μA cm^{-2}). The value of b_a changed slightly between the neat Q235 steel and metal/coating system. However, the absolute b_c values of coatings/metal system were much larger than that of neat Q235 steel (-62.9 mV dec^{-1}), indicating that cathodic reaction (mainly the oxygen reduction reaction) was inhibited when Q235 steel coated with PAA composite coatings.

The protection efficiency of the Q235 steel is calculated using the following equation (1)[39]:

$$P_{EF}\% = \frac{i_{corr}(uncoated) - i_{corr}(coated)}{i_{corr}(uncoated)} \times 100\% \quad (1)$$

Obviously, the P_{EF}% of PAA-2.5%MAT (99.5%) is the highest, suggesting that this composite coating provides better anticorrosion performance on Q235 steel.

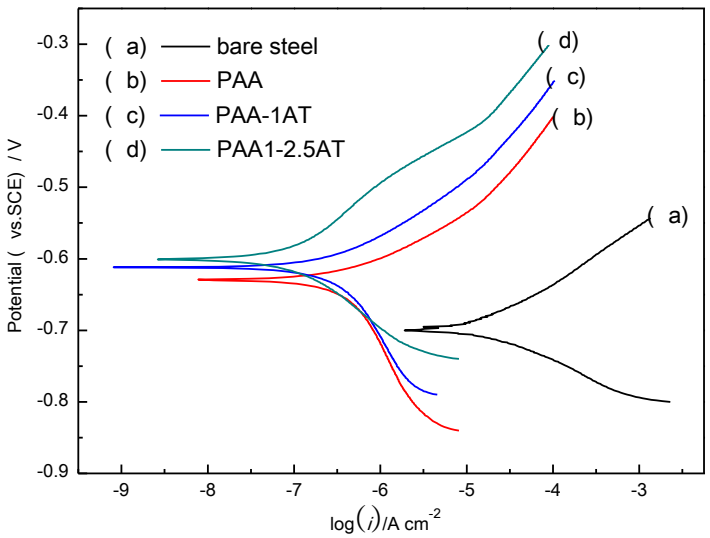

Figure 8. Polarization curves of bare Q235 steel (a), neat PAA coating (b), PAA 1% MTA coating (c) and PAA /2.5% MTA coating (d) immersed in 3.5%NaCl solution after 48 hours.

Table 1. Corrosion parameters of different specimen immersed in 3.5% NaCl solution after 48 hours

	E_{corr}(V/vs.SCE)	i_{corr} (μA cm^{-2})	b_a (mV dec^{-1})	b_c (mV dec^{-1})	R_p (KΩcm^2)
Q235 steel	-0.701	17.1	74.3	-62.9	1.94
PAA	-0.635	0.72	81.5	-241.3	46.2
PAA/1 %MTA	-0.614	0.12	95.7	-187.5	280
PAA/2.5%MTA	-0.601	0.082	91.2	-152.5	495

3.5 EIS measurements

To investigate the anticorrosive performance and degradation processes of Q235 steel coated with pure PAA and PAA/MTA composite coatings, impedance diagrams (including Nyquist and Bode plots) were conducted at OCP after different immersion time in 3.5% NaCl solution, and presented in Figure 9.

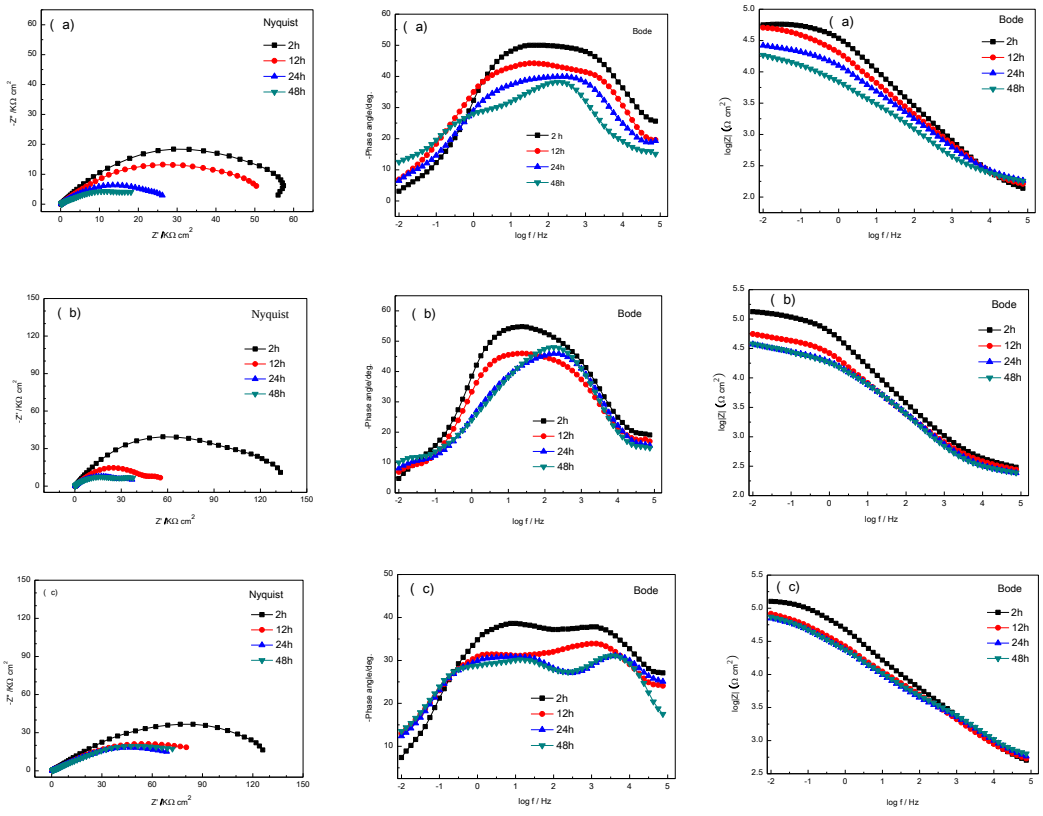

Figure 9. EIS spectrum obtained after different immersion times in 3.5%NaCl solution by PAA coating(a), PAA-1% MTA (b) and PAA-2.5 % MTA coating (c).

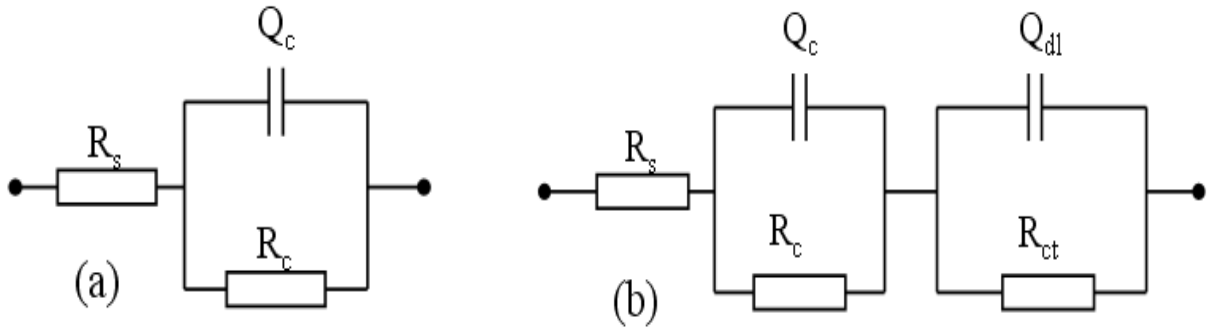

Figure 10. Equivalent circuits of Q235 steel/aromatic acrylate coatings in 3.5wt% NaCl solution, (a): for one time constant; (b): for two time constants.

Table 2. The electrochemical corrosion parameters fitted from the equivalent circuit

coatings	Time hour	R_s Ω cm^2	Q_c μF cm^{-2} Hz$^{1-n_1}$	n_1	R_c KΩ cm^2	Q_{dl} μF cm^{-2} Hz$^{1-n_2}$	n_2	R_{ct} KΩ cm^2
PAA	2	0.01	6.61	0.69	65.1			
	12	0.01	1.25	0.53	1.45	1.61	0.74	4.01
	24	0.01	1.43	0.99	0.56	21.5	0.52	3.29
	48	0.01	55.6	0.59	0.49	0.73	0.85	2.63
PAA	2	0.01	3.89	0.66	141			
1%MTA	12	0.01	9.87	0.87	31.2	8.91	0.59	46.7
	24	0.01	9.59	0.59	30.4	41.1	0.74	42.1
	48	0.01	7.06	0.63	17.2	60.1	0.69	41.4
PAA	2	0.01	5.31	0.51	23.4	1.37	0.71	131
2.5%MTA	12	0.01	9.57	0.55	21.2	6.48	0.55	89.6
	24	0.01	4.23	0.51	4.42	12.8	0.57	89.1
	48	0.01	1.56	0.65	3.85	16.5	0.54	87.1

For the neat PAA coatings (Figure 9a), only one time constant can be observed after 2 hours immersion and the impedance modulus is high, suggesting the good corrosion resistance performance at the initial immersion. The impedance modulus in the low frequency decreased gradually with the increase of immersion time and two time constants appeared after 12 hours, indicating corrosion medium (such as water, Cl^- and oxygen) permeated into the coating and reacted with the substrate metal. For the PAA coatings with 1 wt% and 2.5 wt% MTA (Figure 9b and 9c), the diagrams also presented two time constants. The impedance modulus decreased quickly during the initial 12-hour immersion and then remained stable during the longer immersion times. The capacitive arc radiuses of MTA containing PAA coating are much larger than that of neat PAA coating, suggesting the existence of oligoaniline improved the corrosion resistance of PAA coating.

In order to quantitative evaluate the degradation processes of the composite coatings, two equivalent circuits (Figure10a and 10b) were used to fit the EIS data and the corrosion parameters obtained from ZSimpWin 3.21 software were summarized in Table 1. In Figure10, R_s is the solution resistance, constant phase angle element Q is used instead of pure capacitance, because a dispersion effect may be caused between the metal/coating system [40,41]. Q is expressed as $\omega\text{-}n/Y_0\cdot(\cos n\pi/2 + j \sin n\pi/2)$, where Y_0 and n are the constant and exponent, respectively, and ω is the angular frequency in rad s^{-1} ($\omega = 2\pi f$), and $j^2 = -1$ is an imaginary number. The high-frequency elements Q_c~ R_c correspond to the capacitance and coating resistance of composite coating; The medium-low frequency elements Q_{dl}~R_{ct} are double-layer capacitance and charge-transfer resistance, respectively[42-46].

As shown in Table 2, R_s kept unchanged during the whole immersion time. The coating resistance (R_c) of PAA/ MTA coatings were higher than the neat PAA coating from 2 to 48 hours immersion. Especially, the PAA coating containing 1% MTA owned a maximum value, which varied from 141 to 17.2 KΩ cm^2. With the addition of MTA, the porous PAA coating was improved and as time passed, the accumulation of the corrosive ions into the porosities of PAA coating lead to the higher affinity to ions and became more conductive. Thus, the R_c of the three coatings decreased with the increase of immersion time in 3.5% NaCl solution.

In case of PAA coating containing different content of MTA, both of the R_c and the charge-transfer resistance (R_{ct}) decreased with time. The R_{ct} of the neat PAA coating, PAA coating containing 1% and 2.5% MTA, reduced from 4.01 to 2.63 KΩ cm^2, 46.7 to 41.4 KΩ cm^2, 89.6 to 87.1 KΩ cm^2 from 12 to 48 hours, respectively. Moreover, the PAA coating containing 2.5% MTA exhibited the best corrosion resistance, probably due to the conductivity and chelation of MTA. On the one hand, the anodic and cathodic reaction can be insulated because the presence of MTA facilitated metal oxide film formation; On the other hand, the metal chelating substance and the shielding effect of oxygen from MTA could also improve the anti-corrosion effect of PAA coating.

4. CONCLUSION

In summary, we have been successfully prepared electroacitve oligoaniline based coatings by photocuration of hexafunctional acrylate with MTA. Electrochemical measurements indicate that MTA obviously enhanced corrosion protection efficiency of PAA coating based on Q235 carbon steel. The protection efficiency PAA-2.5%MAT increased to more than 99%. This electroactive and photocurable oligoaniline showed promising applications for anticorrosion coatings.

ACKNOWLEDGEMENTS

This research is supported by Open Foundation Grant LMMT-KFKT-2014-008 from Key Laboratory of Marine Materials and Related Technologies, Ningbo Natural Science Foundation (2015A610016) and National Science Foundation of China (41506098).

References

1. D.W. DeBerry, *J. Electrochem. Soc*., 132(1985)1022.

2. J.G. Wang, *Synth. Met*., 132(2002)53.
3. U. Riaz, C. Nwaoha, S.M. Ashraf and R.L. Mat. *Prog. Org. Coat*., 77(2014) 743.
4. H. Lu; B. Zeng. *Pain.coat. ind*., 37(2007)50.
5. L. Qin, W. Zhao, H. Hou, Y. Jin, Z. Zeng, X. Wu, X. Wu. L Qin, W Zhao, H Hou, Y Jin, Z Zeng and X Wu, *RSC Adv*., 4(2014) 60307.
6. J.L. Camalet, J.C. Laccroix, S.Aeiyach, K.I.C. Ching and P.C. Lacaze, *Synth. Met*., 102(1999)1386.
7. A. Guenboure, A. Kacemi and A. Benbachir, *Prog. Org. Coat.*, 39(2000)151.
8. S. Pour-Ali, C. Dehghanian and A. Kosari, *Corros. Sci.*, 90(2015) 239.
9. N. Wang, Y. H. Wu, K. Q. Cheng and J. Zhang, *Mater. Corros*., 65(2014)968.
10. L. Ma, F.F. Chen, Z.T. Li, M.Y. Gan, J. Yan and S.J. Wei, *Compos. Part B Eng.*, 58(2014) 54.
11. C. J. Weng, C. H. Chang, I. L. Lin, J. M. Yeh, Y. Wei and C. L. Hsu, *Surf Coat Technol.*,, 207(2012)42.
12. E. Akbarinezhad, M. Ebrahimi, F. Sharif and A. Ghanbarzadeh,*Prog Org Coat.*, 77(2014) 1299.
13. A. H. Navarchian, M. Joulazadeh and F. Karimi, *Prog Org Coat.*, 77(2014)347.
14. A. Olad and R. Nosrati, *Prog Org Coat.*, 76(2013)113.
15. A. Olad, M. Barati and S. Behboudi, *Prog Org Coat.*, 74(2012)221.
16. Y.S. Hao, F.C. Liu and E. H. Han, *Prog Org Coat.*, 76 (2013)571.
17. Z.T. Li, L.Ma, W.L. Li, M.Y. Gan, W. Qiu and J. Yan, Polym. *Adv. Technol.*, 24(2013)847.
18. P.P. Deshpande, S.S. Vathare, S.T. Vagge, E. Tomsik and J. Stejskal, *Chem. Pap.*, 67(2013)1072.
19. E. Akbarinezhad, *J. Supercrit. Fluids.*, 94(2014)8.
20. K.C.Chang, C.H. Hsu, H.I. Lu, W.F. Ji, C.H. Chang and W.Y. Li, *Express. Polym. Lett.*, 8(2014)243.
21. R. Arukula, A.R. Thota, C.R.K. Rao, R. Narayan and B. Sreedhar, *J. Appl. Polym. Sci.*, 131(2014)40794.
22. H. Cui, Y. Wang, L. Cui, P. Zhang, X. Wang and Y. Wei,*Biomacromolecules.*, 15(2014) 3146.
23. C.J. Weng, C.H. Chang, C.W. Peng, S.W. Chen, J.M. Yeh and C. L. Hsu, *Chem. Mater.* , 23(2011) 2075.
24. K.Y. Huang, C.L. Shiu, P.S. Wu, Y.Wei, J.M. Yeh and W.T. Li, *Electrochim. Acta.*, 54(2009)5400.
25. K.Y. Huang, Y.S. Jhuo, P.S. Wu, C.H. Lin, Y.H. Yu and J.M. Yeh, *Eur. Polym. J.*, 45(2009)485.
26. K.C.Chang, H.I.Lu, C.W.Peng, M.C. Lai, S.C. Hsu and M.H. Hsu, *ACS Appl. Mat. Interfaces.*, 5(2013)1460.
27. T.C. Yeh, T.C. Huang, H.Y. Huang, Y.P. Huang, Y.T. Cai and S. T. Lin, *Polym Chem.*, 3(2012) 2209.
28. S.C. Lin, C.S. Wu, J.M. Yeh and Y.L. Liu, *Polym Chem*.,5 (2014) 4235.
29. H. Y. Hang, T. C. Huang, T. C. Yeh, C. Y. Tsai, C. L. Lai and M. H. Tsai, *Polym.*, 52(2011)2391.
30. L. Gu, S. Liu, H.C. Zhao and H. B. Yu, *RSC Adv*., 5(2015)56011.
31. H. Strub, *Actual Chim.* , 5(2000)13.
32. Z. Y. Wang, C. Yang, J. P. Gao, J. Lin, X. S. Meng and Y. Wei, *Macromol.*, 1998, 31, 2702.
33. P.J. Kinlen, Y. Ding and D.C. Silverman, *Corros.*, 58 (2002) 490
34. Z. Deng, W.H. Smyrl, and H.S. White, *J. Electrochem. S*oc., 36, (1989)2152
35. V. Brusic, M. Angelopulos and T. Graham, *J.Electrochem. Soc*., 144 (1997) 436.
36. V.J.Gelling, M.M. Wiest, D.E. Tallman, G.P. Bierwagen and G.G. Wallace, *Prog. Organic Coatings*, 43(2001)149
37. A. M. Mathew and P. Predeep, *Prog. Org. Coat.*, 74(2012) 14.
38. X. Zhao, S. Liu and B.R. Hou, *Appl. Mech. Mater.*, 599-601(2014)40-43.
39. C.J. Weng, C.H. Chang, C.W. Peng, S.W. Chen, J.M. Yeh, C.L. Hsu and Y. Wei. *Chem. Mater.*, 23(2011) 2075.
40. H.Y. Sun, S. Liu and L.J. Sun, *Int. J. Electrochem. Sci.*, 8(2013)3494.
41. S. Liu, H.Y. Sun, L.J. Sun and H.J. Fan, *Corros. Sci*., 65(2012)520.
42. Q.L.Cheng and Z. Y. Chen, *Int. J. Electrochem. Sci.*, 8(2013)282.
43. E. M. Sherif and A. A. Almajid, Int. J. Electrochem. Sci., 10(2015)34.
44.. X. Zhao, S. Liu, Z.J. Cai, B.R. Hou. *Chin. J. Oceanol. Limnol.*, 33(2014)1163.

45. M. A. Alam, El-Sayed M. Sherif and S. M. Al-Zahrani, *Int. J. Electrochem. Sci*., 8 (2013) 3121.
46. L. Gu, S. Liu, H.C. Zhao and H. B. Yu, *ACS Appl. Mater. Interfaces*., 7(2015)17641.